THE JOURNAL OF PHYSICAL CHEMISTRY B
A JOURNAL OF THE AMERICAN CHEMICAL SOCIETY

pubs.acs.org/JPCB

Article

Distinctive Formation of PEG-Lipid Nanopatches onto Solid Polymer Surfaces Interfacing Solvents from Atomistic Simulation

James Andrews and Estela Blaisten-Barojas*

Cite This: https://doi.org/10.1021/acs.jpcb.1c07490

Read Online

ACCESS | Metrics & More | Article Recommendations | Supporting Information

ABSTRACT: The interface between solid poly(lactic acid-*co*-glycolic acid), PLGA, and solvents is described by large-scale atomistic simulations for water, ethyl acetate, and the mixture of them at ambient conditions. Interactions at the interface are dominated by Coulomb forces for water and become overwhelmingly dispersive for the other two solvents. This effect drives a neat liquid-phase separation of the mixed solvent, with ethyl acetate covering the PLGA surface and water being segregated away from it. We explore with all-atom Molecular Dynamics the formation of macromolecular assemblies on the surface of the PLGA-solvent interface when DSPE-PEG, 1,2-distearoyl-sn-glycero-3-phosphoethanolamine-*N*-(polyethylene glycol)$_n$ amine, is added to the solvent. By following in time the deposition of the DSPE-PEG macromolecules onto the PLGA surface, the mechanism of how nanopatches remain adsorbed to the surface despite the presence of the solvent is probed. These patches have a droplet-like aspect when formed at the PLGA-water interface that flatten in the PLGA-ethyl acetate interface case. Dispersive forces are dominant for the nanopatch adhesion to the surface, while electrostatic forces are dominant for keeping the solvent around the new formations. Considering the droplet-like patches as wetting the PLGA surface, we predict an effective wetting behavior at the water interface that fades significantly at the ethyl acetate interface. The predicted mechanism of PEG-lipid nanopatch formation may be generally applicable for tailoring the synthesis of asymmetric PLGA nanoparticles for specific drug delivery conditions.

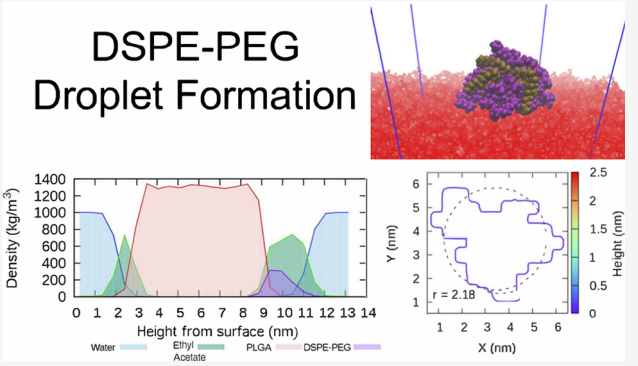

1. INTRODUCTION

Soft-matter materials and polymers are widely used in the controlled delivery of drugs. Polyethylene glycol (PEG) and the macromolecule DSPE-PEG (1,2-distearoyl-*sn*-glycero-3-phosphoethanolamine-*N*-(polyethylene glycol)$_n$amine) formed by the DSPE phospholipid bonded to the PEG polymer are widely used in nanoparticle construction and may modify the nanoparticle surfaces aiding the formation of micelles, disks, vesicles, and bilayers that are commonly assembled for therapeutic drug delivery. However, the nanoparticle assembly mechanism as well as the amalgamation of PEGylated macromolecules onto their surfaces are not well understood at the atomic level.[1−4] PEG is a biocompatible polymer widely used in controlled drug release. The attachment of PEG onto the surface of nanoparticles is known as PEGylation and is shown to improve the therapeutic potency.[5−7] In particular, PEG(2000) and its lipid block copolymer DSPE-PEG(2000) is a PEGylated phospholipid soluble in water and is frequently used in nanomedicine for the fabrication of lipid-polymer hybrid nanoparticles, liposomes, and microemulsions because the end-terminal functional groups can be functionalized with a variety of organic and inorganic molecules.[8−11]

An interesting formation of heterogeneous patches on the surface of poly(lactic acid-*co*-glycolic acid), PLGA, nanoparticles has been reported in the literature.[8,12,13] These formations may enhance the nanoparticle fixation specificity of the drug ported by the nanoparticles. Computational modeling efforts of deposited PEGylated block polymers on a nanoparticle's surface have been attempted at the coarse-grained level[8] showing that the hydrophobic DSPE tails had a tendency to agglomerate. Other experimental works[2,14] hypothesize that, in aqueous solutions, the PLGA nanoparticles are enveloped by a bilayer membrane of DSPE while DSPE-PEG(2000) macromolecules collapse into the nanoparticle surface in discontinuous spots. It is additionally believed that DSPE-PEG(2000) macromolecules interact preferentially with the lactic monomers of PLGA. This macromolecule is referred to as DSPE-PEG, therein. Simulation and modeling provide insight at the atomic scale enabling a level of control and detail unavailable to experiments. PEG(2000) has been studied

Received: August 23, 2021
Revised: November 1, 2021

Table 1. Composition, Size, and NPT Equilibration Methods of the MD-Simulated Systems

system	No. of atoms	No. of molecules	NPT equilibration	time (ns)
PLGA slab	21 696	32 PLGA	semi-isotropic Berendsen	100
PLGA + water	42 432	32 PLGA	Berendsen	5
		6912 water	Parrinello-Rahman	100
PLGA + ethyl acetate	69 828	32 PLGA	Berendsen	5
		3438 EA	Parrinello-Rahman	100
		32 PLGA		
PLGA + EA:water	46 500	603 EA	Berendsen	5
		5454 water	Parrinello-Rahman	100
DSPE-PEG	452	1 DSPE-PEG		
in vacuo	1808	4 DSPE-PEG		
	21 188	1 DSPE-PEG		
		6912 water		
DSPE-PEG + water			Berendsen	5
	37 808	4 DSPE-PEG	Parrinello-Rahman	10
		12,000 water		
	28 452	1 DSPE-PEG		
		2000 EA	Parrinello-Rahman	
DSPE-PEG + ethyl acetate			pressure decrease	8
	225 808	4 DSPE-PEG	Parrinello-Rahman	12
		16 000 EA		
		32 PLGA		
	40 976	6276 water		
		1 DSPE-PEG		
PLGA + water + DSPE-PEG			Berendsen	5
	42 332	32 PLGA	Parrinello-Rahman	10
		6276 water		
		4 DSPE-PEG		
		32 PLGA		
	66 598	3175 EA		
		1 DSPE-PEG		
PLGA + EA + DSPE-PEG			Berendsen	8
		32 PLGA	Parrinello-Rahman	12
	40 010	1179 EA		
		4 DSPE-PEG		
		32 PLGA		
	46 480	5362 water		
		589 EA		
		1 DSPE-PEG		
PLGA + EA/water + DSPE-PEG			Berendsen	5
		32 PLGA	Parrinello-Rahman	20
	48 308	603 EA		
		5454 water		
		4 DSPE-PEG		

computationally both in solvents and its condensed phases.[15] Meanwhile, DSPE-PEG has received less attention in the literature, with few examples such as the determination of micelle formation in concentrated aqueous salt solutions simulated using the CHARMM force field[11] to a pileup deposition modeled with the MARTINI coarse-grained force field.[8]

Our paper elucidates the mechanism of anisotropic formation of DSPE-PEG nanopatches on 200−500 nm sized PLGA(50:50) nanoparticles in the presence of various solvents at the atomic scale. The glassy condensed phase of PLGA(50:50) has been successfully modeled and validated against experiments in our group.[16] For convenience, in what follows PLGA(50:50) is termed PLGA. The solid PLGA surface is here thoroughly inspected when interfacing three different solvents, namely, water, ethyl acetate (EA), and the mixture of EA/water with a concentration of 1:1.849 by mass commonly used in syntheses experiments.[8,12,13] Furthermore, the fate of solvated DSPE-PEG macromolecules is followed in time yielding aggregation and formation of localized aggregates adsorbed on the PLGA surface-solvent interface that resemble "droplets". We investigate these macromolecular aggregates in the solvents and their deposition on the PLGA surface. The study emphasizes the solvent effects on the variety of droplets that form on the PLGA surface. Thus, our studied heterogeneous nanocomposite has three ingredients, namely, a solid polymer slab of PLGA with its surface interfacing a solvent in which four solvated DSPE-PEG macromolecules, first aggregate and lately deposit onto the PLGA surface acquiring a drop-like structure. The hydrophilic head of the DSPE lipid is functionalized with PEG(2000), while the two acyl chains remain as the macromolecule hydrophobic tail.

The paper is organized as follows. The Models and Methods section provides a detailed description of how this heterogeneous system is built at the atomic scale and extensive insight on the all-atom Molecular Dynamics (MD) large-scale simulation methodology. The Results and Discussion section provides analyses of the PLGA surface interfacing with each of the three solvents studied and probes the fate that solvated DSPE-PEG macromolecules undergo when reaching the PLGA-solvent interface. In all cases the macromolecules adhere to the surface, morphing into a patch aggregate resembling a droplet. An inspection into the droplet-like patch characteristics is also included. The Conclusion section summarizes the observations and provides a critical discussion of the formation of these macromolecular structures on the surface. Quantitative details are provided in the Supporting Information.

2. MODELS AND METHODS

We set up 14 different composite systems, either binary, ternary, or quaternary, composed of a PLGA solid slab, liquid water, liquid ethyl acetate, and solvated PEG-lipid macromolecules. Table 1 summarizes the composition of each system

https://doi.org/10.1021/acs.jpcb.1c07490
J. Phys. Chem. B XXXX, XXX, XXX−XXX

providing their number and type of molecules, system total number of atoms, and MD equilibration methodology.

The PLGA polymer matrix was built with 32 PLGA copolymer macromolecules, each of them composed of 45 lactic acid monomers ($-COCHCH_3O-$) and 45 glycolic acid monomers ($-COCH_2O-$) with a random distribution along the polymer chain.[17] The molecular weight of each polymer macromolecule was 5872 u, comprised 678 atoms, and was terminated with a hydroxyl radical bonded to the lactic acid monomer at one end and a saturated glycolic acid monomer at the opposite end. Two lactic acid stereoisomers, L- and D-, with a 50:50 mixing ratio were included randomly distributed in each polymer chain, as has been evidenced experimentally.[18,19] Our polymer matrix was amorphous, consistent with experiment.[20] Modeling of the PLGA macromolecules was performed with the General AMBER Force Field (GAFF)[21] implemented with custom-generated restrained electrostatic potential (RESP)[22] atomic charges as described in detail in our previous work.[16,17] Bonding terms were represented by Morse potentials.

DSPE-PEG has the chemical formula of $(C_2H_4O)_{45}C_{42}H_{83}N_2O_9P$, 2773.5 u molecular weight, and contains 452 atoms. Figure S1 of the Supporting Information depicts this PEG-lipid macromolecule, a block copolymer structure. Modeling of the DSPE-PEG macromolecule was achieved by GAFF combined with the AMBER-Lipids17 force field[23] with custom-generated RESP atomic charges. Bonding terms were represented by Morse potentials. The newly generated atomic charges were calculated based on the hybrid B3LYP 6-31G*hybrid density functional theory (DFT) approach and the Merz-Singh-Koleman population analysis[24,25] for obtaining the electrostatic potential (ESP) charges as implemented in Gaussian 09.[26] This task entailed first porting the DFT-ESP atomic charges to the AmberTools 2018 Antechamber[27,28] utility for conversion into RESP charges and, second, converting the AMBER topology file into files consistent with the GROMACS 2018−2020 package[29] via the Python API ParmEd.[30] Our custom RESP approach diminishes the overpolarization afforded by the Hartree−Fock with 6-31G* basis set approach.[31] Figure S2 of the Supporting Information depicts the RESP atomic charges for DSPE-PEG, and Table S1 provides their values.

For the solvents considered in this work, water was simulated with the SPC/E model,[32] and EA molecules ($CH_3COOCH_2CH_3$) were modeled with GAFF using custom RESP charges from previous calculations.[15,16]

The generation of the heterogeneous system of a PLGA surface interfacing with different solvents entailed the preparation of the PLGA solid surface, which was based on our previous work on both PLGA in the condensed phase[17] and the associated computational workflow.[33] The Molecular Dynamics simulations were done with the GROMACS 2018−2020[34−36] package using a 1 fs time step, 1.4 nm cutoff, periodic boundary conditions (PBC), and PME[37] long-range electrostatic corrections. Table 1 provides the specifics of the system size. The solid PLGA sample was prepared by setting an initial cubic computational box with the 32 PLGA macromolecules. The initialization protocol in each system listed in Table 1 consisted in optimizing via a global minimization, followed by several 5 ns NVT runs at escalating temperatures to reach 300 K. Subsequently, the 20 ns NPT MD equilibration at 300 K and 101.325 kPa yielded a PLGA equilibrium density of 1306 kg/m^3 in agreement with commercial products.[38] The velocity-rescaling temperature[39] and the Berendsen pressure[40] couplings were used followed by a 100 ns semi-isotropic NPT re-equilibration process in which two directions were held against walls resulting in a prismatic rectangular slab of solid PLGA with two smoothened opposite faces of area 6.2 × 6.2 nm by a height of 7.2 nm. Even smooth, the PLGA slab opposite sides were formed by the disordered, entangled macromolecules of the bulk system with protruding macromolecular formations involving portions of approximately half of the slab macromolecules. These two molecularly built slab cross sections were far from being flat-unstructured surfaces. Since PBC was applied, the simulation mimicked an extended PLGA surface with no curvature, a reasonable consideration for the study of localized mechanisms on 200−500 nm nanoparticles,[8,12,13] as the one we addressed in this paper.

The PLGA solid slab was placed at the bottom of a taller prismatic box 6.2 × 6.2 × $h_{solvent}$ nm with the two PLGA slab smoothened faces interfacing with the solvent. The computational box hight $h_{solvent}$ was 11.6 nm for water, 20.2 nm for EA, and 13.0 nm for the mixed solvent. The complete model systems for analysis of the PLGA-solvent interface emulated the components of the experimental synthesis environment[8,12,13] with system sizes listed in Table 1 along the NPT equilibration methodology. Solvent molecules were initially placed randomly in the above-described computational box within the space not already occupied by the PLGA solid slab. These systems were equilibrated by a sequence of NPT MD Berendsen and Parrinello-Rahman[41,42] runs at T = 300 K and 101.325 kPa rendering solvent densities of 1000 kg/m^3 for water, 907 kg/m^3 for EA, and a liquid phase-separated mixed EA/water solvent in an equilibrated volume of 497 nm^3 including the PLGA slab. As an example, Figure 1 depicts the equilibrated PLGA slab immersed in water and in the EA/water solvent that displayed liquid-phase separation.[16] Results and discussion are included in Section 3.1.

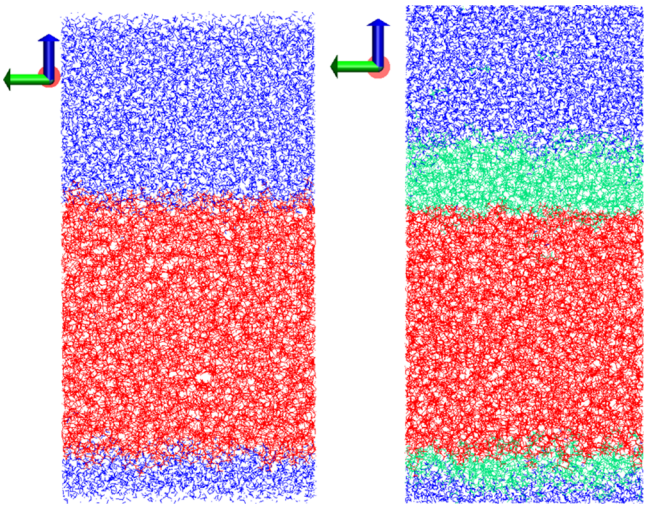

Figure 1. Illustration of the equilibrated PLGA solid slab (red) interfacing solvents, either water (blue) or EA (green). (left) Solvent is water within a prismatic volume of 6.2 × 6.2 × 11.6 nm. (right) Solvent is mixed EA/water within a volume of 6.2 × 6.2 × 13 nm. Cartesian axes are X (red), Y (green), and Z (blue). Depicted configuration corresponds to one saved frame in which the coordinates of all atoms are written to the file, 42 432 in the case of water and 46 500 in the mixed EA/water solvent.

https://doi.org/10.1021/acs.jpcb.1c07490
J. Phys. Chem. B XXXX, XXX, XXX−XXX

Solutions of a single DSPE-PEG macromolecule and a group of four of them solvated in water and in EA were addressed as detailed in Table 1. For the aqueous solution two successive Berendsen followed by Parrinello Rahman NPT MD simulations were undertaken. For the EA solutions, five NPT preparation runs with the Parrinello-Rahman barostat brought the system from 10 to 5, 2.5, 1 MPa and, finally, to 101.325 kPa through 2 ns concatenated runs and a final 12 ns equilibration run. On the one hand, the aqueous solution showed that DSPE-PEG macromolecules aggregate and collapse in globular structures. On the other hand, the one-macromolecule EA solution displayed an extended polymer−lipid chain, which led to selecting a large system size for the four-macromolecule solution as shown in Table 1. These solutions acquired densities similar to the pure solvents, 999 ± 0.1 and 906.3 ± 0.1 kg/m^3 for water and EA, respectively, as described in Section 3.2.

A similar in silico protocol was followed for the highly heterogeneous PLGA + solvent + DSPE-PEG ternary and quaternary composite systems listed in Table 1. Initially the DSPE-PEG single or clustered structures obtained in solution were placed close to the PLGA surface in three different orientations. Equilibration was achieved by applying Berendsen followed by Parrinello-Rahman NPT MD as indicated in Table 1. An alternative approach was adopted as described in Section 3.3.

Once the heterogeneous systems were NPT-equilibrated, for the study of solute properties and properties between system components depending on distances between atoms, it was necessary to keep the system volume fixed, without the volume fluctuations afforded in the NPT MD methodologies. Therefore, after systems listed in Table 1 were NPT MD-equilibrated, extensive 50−200 ns NVT MD simulations were undertaken on each of them for data collection at T = 300 K and the corresponding equilibrated densities of bulk slab interfacing the solutions. Data were collected during the last 20−40 ns for the analyses.

Multiple custom scripts and programs in Python and Fortran were developed for postanalysis calculations including the individual polymers potential energy, their interaction energy with the solvent, the PLGA structural properties, the macromolecular cluster properties, the distances distribution functions, the droplet mass distribution, and wetting contact angle. Interaction energies entailed using the GROMACS *rerun* feature[29] that enabled the energy calculation from the MD saved trajectory. For the PLGA-solvent system described in Section 3.1, the interaction energy was calculated as $E_{int} = E_{total} - (E_{PLGA} + E_{solvent})$ by isolating atoms belonging to PLGA into a file, atoms belonging to solvent molecules in a separate file, and independently recalculating their energies with the *rerun* feature. This approach yielded, separately, the energies of each subsystem recalculated from the exact same positions as they had when calculated together along the trajectory. The methodology was exploited again in Section 3.2 for the calculation of the interaction energies of the solvated DSPE-PEG macromolecules with the solvent, $E_{int} = E_{total} - (E_{macromolecules} + E_{solvent})$. In Section 3.3 the protocol was used again for the interaction energy of the solid PLGA slab and the DSPE-PEG macromolecular droplet formed in solvents, $E_{int} = E_{PLGA+droplet} - (E_{PLGA} + E_{droplet})$, with $E_{PLGA+droplet}$ being the energy of the PLGA solid slab and the DSPE-PEG macromolecules kept together in one isolated file, pure PLGA in another file, and pure macromolecular droplet in a third file. Furthermore, the interaction energy that kept the DSPE-PEG macromolecules forming droplets was $E_{int} = E_{droplet} - (E_1 + E_2 + E_3 + E_4)$, where E_1 through E_4 were the potential energy of each DSPE-PEG macromolecule isolated in a separate file. Along these special reruns, GROMACS outputs the contribution to the calculated energies from each force field potential function. On the basis of this useful approach, nonbonded dispersive (Lennard-Jones) and electrostatic (Coulomb) energies between the separated system components were amenable to be recorded and reported.

3. RESULTS AND DISCUSSION

3.1. PLGA-Solvent Interface. At T = 300 K the PLGA slab interfacing solvent was at a temperature below its glass transition,[17] remaining solid while in contact with the solvents along the full in silico experiment. We characterized the PLGA-solvent interface by a width of 1.5 nm within which PLGA monomers and solvent molecules coexisted. Interfacing regions of that width are characteristic of polymeric surfaces enabling the accommodation of solvent molecules on a rough surface. Within the interface region, the PLGA solid block exposed 480 lactic and glycolic acid monomers to the solvent molecules with 4% of them being end monomers of the PLGA macromolecules. Figure 2 shows the system density profile evidencing the PLGA-solvent interface; the abscissa in the figure depicts the height of different slices of matter parallel to the solid−liquid interfacing plane. Additionally, Figure 2 is instrumental in validating that the interface region has, indeed, a 1.5 nm width in all three solvent cases. Figure 2a,b shows the density profile of the PLGA-water and PLGA-EA systems. In the mixed EA/water system the two liquids phase-separated with the EA shielding the solid surface from the water. The liquid phase separation was evidenced clearly in the density profile of the system shown in Figure 2c. Therefore, the interaction of PLGA-EA was definitely preferred by the system when compared to that of PLGA-water. MD simulations are orders of magnitude shorter compared to laboratory times that would allow PLGA nanoparticles to undergo a hydrolysis or dissolution in the buffer solvents where they were synthesized. In fact, PLGA nanoparticles in the wet laboratory are collected, dried, and washed without breaking apart.[8,12,13]

The proximity of solvent molecules to the surface was determined from the distribution of atomic distances between the PLGA slab atoms and solvent molecule atoms within the 1.5 nm interface thickness as depicted in Figure 3. For water, a first layer of water molecules between 0.2 and 0.4 nm was clearly identified in Figure 3a, while a broadly spread second layer was resolved between 0.5 and 0.7 nm. The mini-peak at ∼0.17 nm was primarily due to hydrogen bonds formed between water oxygen atoms and the hydrogen of the end PLGA monomer hydroxyl group. Figure 3b depicts the distribution of atomic distances between the PLGA surface and the EA molecules within the interface region displaying an extended first coordination shell, while this effect is absent in water. In addition, hydrogen bonds did not form due to EA. Figure 3c illustrates the distribution of atomic distances between the PLGA surface and both water and EA molecules. While the amount of EA molecules close to the surface is comparable to that in the pure EA solvent, the distribution evidenced water molecules in the interfacial region, an artifact of the periodic boundary conditions used in the simulation. In fact, those water molecules were interfacing the lower surface of the PLGA slab as seen in Figure 2c, and this effect would

https://doi.org/10.1021/acs.jpcb.1c07490
J. Phys. Chem. B XXXX, XXX, XXX−XXX

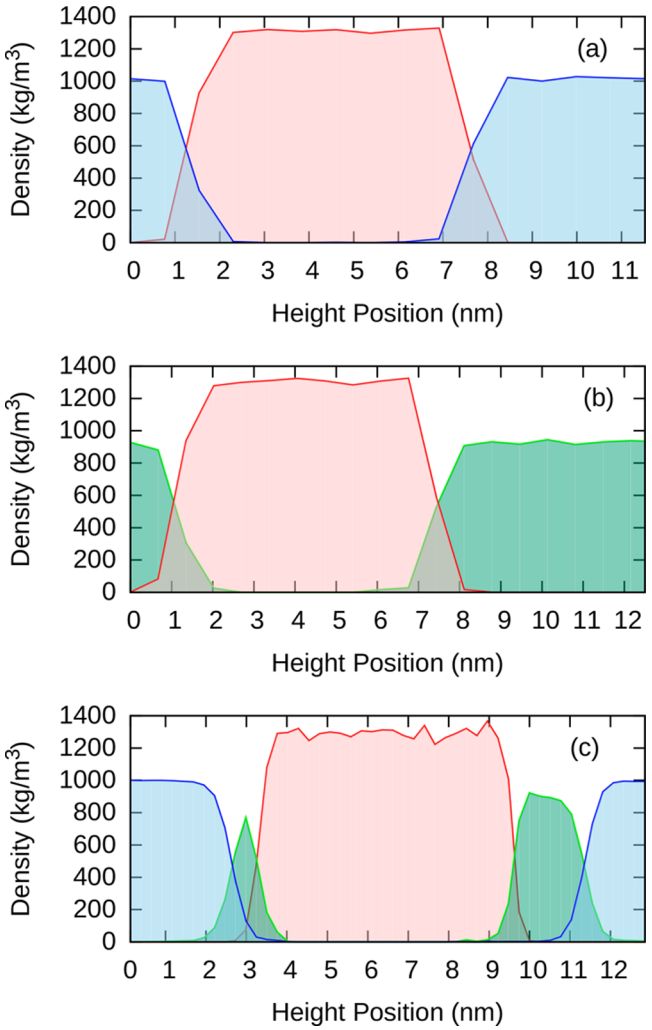

Figure 2. Density profile of the PLGA-solvent system across the computational box. (a) PLGA-water; (b) PLGA-EA; (c) PLGA-mixed EA/water. Color scheme identifies pink as PLGA, green as EA, and light blue as water. The abscissa corresponds to the computational box height. Note: in (b) the height is depicted only up to 12 nm.

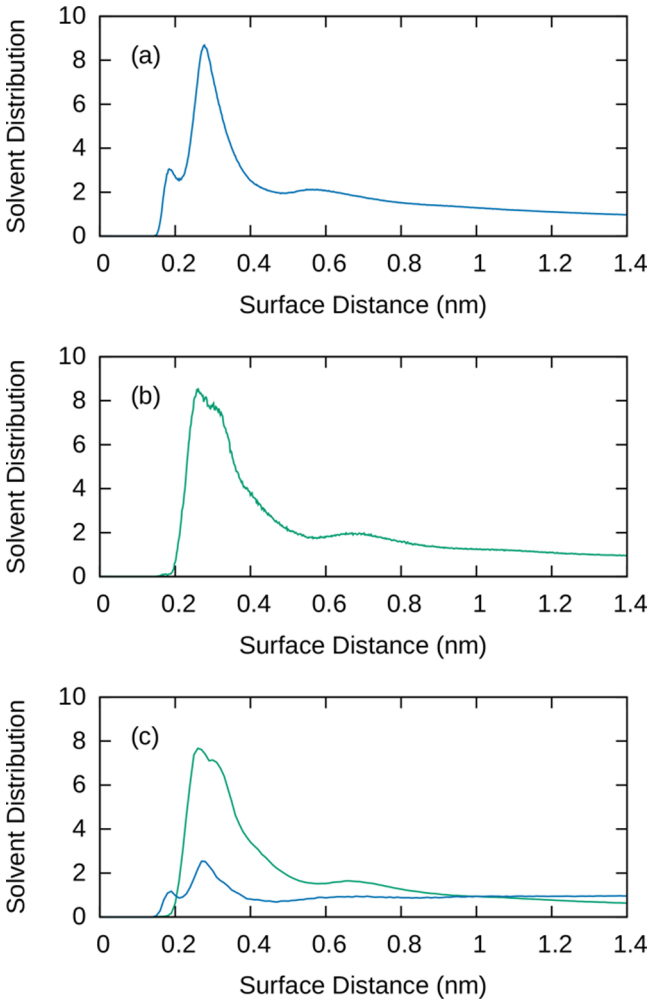

Figure 3. Distribution of atomic distances between PLGA solid slab atoms and solvent atoms within the interface region at 300 K. (a) Water; (b) EA; (c) mixed solvent EA/water. water is in blue, and EA is in green. Data were averaged over the last 20 ns of the NVT simulation. The number of atoms in the interface region and its volume were used in the normalization.

not be present if the amount of solvent molecules had doubled. Even so, the distribution of each participating liquid in the mixed solvent was similar to that shown in Figure 3a,b.

Looking into the energetics between a solid slab and solvents in the interfacial region, the interaction energy of PLGA-solvent for matter in the interface region, $E_{int} = E_{total} - (E_{PLGA} + E_{solvent})$, was E_{int}/atom = -0.27 ± 0.01, -0.16 ± 0.01, and -0.23 ± 0.01 kJ/mol, for water, EA, and mixed solvent, respectively. In water the contribution to this energy was strongly electrostatic (Coulomb) by 67%, while the remaining portion pertained to dispersive interactions (Lennard-Jones). By contrast, in pure EA and mixed EA/water cases the dispersive term was overwhelmingly dominant accounting for 81% and 78% of the total, respectively. We had previously observed this energetics behavior in solutions of the same solvents with solutes being either shorter PLGA molecules[16] or PEG(2000)[15] and attributed the effect to the high polarizability of water when compared to that of EA.

3.2. Fate of Solvated DSPE-PEG Macromolecules. A battery of simulations was performed for one DSPE-PEG macromolecule in vacuum and when solvated in water, EA, or a mixture of these solvents. NVT MD simulations of the single DSPE-PEG macromolecule at T = 300 K in vacuum was run for 5 ns. The solution relative solute concentrations were 2.2% and 1.6% by weight, respectively. Table 2 lists several DSPE-PEG macromolecule structural properties in the different environments. Reported quantities are the mass-weighted radius of gyration R_g, the end-to-end distance R_{ee} between centers of mass of the polymer terminating monomers, the orientational order parameter Z,[43,44] the moments of inertia along the macromolecule principal axes I_A, I_B, I_C, and the solvent-accessible surface area (SASA). The DSPE-PEG macromolecule collapsed into a globule-like cluster both in vacuo and water. However, when solvated in EA the macromolecule R_g doubled in size indicating that the DSPE-PEG was swollen. The order parameter Z describing the randomness of backbone bond orientations with respect to the chain direction vector was approximately zero in all three cases indicating the absence of orientational ordering of backbone angles in this lipid-copolymer. The moments of inertia indicated that the rotational signature of the collapsed macromolecule was a spherical prolate top in all three cases.

In the following step, we inspected the aggregation behavior of four DSPE-PEG macromolecules in the solvents. As a

https://doi.org/10.1021/acs.jpcb.1c07490
J. Phys. Chem. B XXXX, XXX, XXX−XXX

Table 2. Structural Properties of the DSPE-PEG Macromolecule in Various Environments at 300 K[a]

environment	R_g (nm)	R_{ee} (nm)	Z	I_A (u·nm^2)	I_B/I_A	I_C/I_A
DFT	4.18	12.7	0.97	1484	29.9	30.3
		12.9	1.0			
vacuum	0.82 ± 0.02	1.4 ± 0.4	0.2 ± 0.4	935 ± 76	1.2 ± 0.2	1.4 ± 0.2
		1.0 ± 0.4	0 ± 0.4			
water	0.84 ± 0.03	1.2 ± 0.4	−0.1 ± 0.4	983 ± 83	1.3 ± 0.2	1.6 ± 0.2
		1.3 ± 0.5	−0.1 ± 0.4			
EA	1.6 ± 0.3	3.4 ± 1.4	0 ± 0.4	1817 ± 533	3.4 ± 2.2	3.8 ± 2.2
		3.5 ± 1.6	0 ± 0.4			

[a]DFT refers to the DFT optimized structure depicted in Figure S1 of the Supporting Information. The two values of R_{ee} and Z correspond to the property calculated from the head PEG monomer to the terminal carbon atom of each of the two lipid acyl chains. Averages and standard deviations correspond to the last 20 ns of the NVT simulations.

Table 3. Properties of the DSPE-PEG 4-Macromolecules Cluster in Vacuum, Water, and EA at 300 K[a]

	RMSD (nm)	R_g (nm)	I_B/I_A	I_C/I_A	SASA (nm^2)	E_{int} (J/mol)
vacuum	0	1.28 ± 0.01	1.2 ± 0.1	1.4 ± 0.1	56 ± 3	−1306 ± 55
water	0.96	1.32 ± 0.01	1.3 ± 0.2	1.5 ± 0.5	61 ± 2	−1512 ± 82
EA	2.08	2.12 ± 0.11	2.0 ± 0.4	2.4 ± 0.3	137 ± 8	−813 ± 21

[a]RMSD between the final configuration with respect to the vacuum final configuration. Interaction energy between the four cluster macromolecules is $E_{int} = E_{cluster} - \sum_{i=1}^{4} E_{macromolecule_i}$. Averages correspond to the last 20 ns of the NVT MD simulations.

reference, the four DSPE-PEG macromolecules were left to aggregate in vacuum at 300 K along with NVT MD simulation runs resulting in a fairly compact, nearly spherical, cluster after the first nanosecond evolution. The four DSPE-PEG macromolecules solvated in water at relative concentration of 5.1% by mass aggregated displaying properties similar to the cluster in vacuum, albeit they were elongated within the water, resulting in a swollen *premicellar* formation. Micelles containing eight macromolecules and smaller were observed in simulations from a concentrated aqueous solution.[11] Table 3 includes structural details about the incipient micelle assembled in water and shows that this aggregate is significantly more bound than the vacuum-assembled cluster. A subsequent step consisted in solvating the vacuum-formed structure in EA yielding a solute relative concentration of 0.78% by mass. Three independent NPT MD simulations were run, along which the DSPE-PEG macromolecules were loosely packed with R_g twice as large as the aggregate formed in water. These three cluster structures differed between them by more than 1.5 nm root-mean-square deviation (RMSD), while all maintaining an R_g value of 1.9 nm. Such different aggregate structures were initial configurations for the 50 ns NVT MD simulations at 300 K. Along these simulations the DSPE-PEG clusters changed dramatically, only one keeping the four macromolecules loosely aggregated as listed in Table 3. The sporadic aggregation of DSPE-PEG in EA is expected since lipids form micelles in aqueous and basic solvents, preferentially.[45,46]

3.3. DSPE-PEG Nanopatch Formation onto the PLGA Surface. In this Section the PLGA-solvent systems (Section 3.1) are augmented with one or more DSPE-PEG macromolecules added to the solvent region of the computational box in the presence of the PLGA solid slab. First, a single DSPE-PEG macromolecule with a structure acquired in the solutions described in Section 3.2 was placed close to the surface of the PLGA, solvated, NPT equilibrated, and subsequently followed along 100 ns NVT MD at T = 300 K and the corresponding equilibrated density. The solute relative concentration was 2.5% by mass in water and 1.0% by mass in EA. If water is the solvent, the DSPE-PEG macromolecule adheres to the PLGA surface in a compact globular-like structure reminiscent of the collapsed structure obtained in pure water, as shown in Figure 4a. If EA is the solvent,

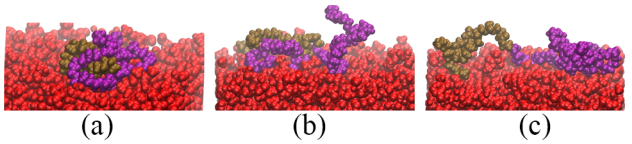

Figure 4. Rendering of the adsorbed DSPE-PEG macromolecule onto the solid PLGA surface within the PLGA-solvent interfacial region at 300 K. Solvent is not depicted: (a) water, (b) ethyl acetate; (c) mixed EA/water solvent.

however, the macromolecule fails to adsorb onto the surface due to its swollen, extended spatial elongation that precludes approaches to the surface. An alternative initial configuration was to retain the structure of DSPE-PEG attached to the PLGA-water surface, remove the water molecules, and replace them by EA molecules or by the mixture of EA/water and re-equilibrate the system. In latter cases the DSPE-PEG macromolecule remained adsorbed to the PLGA surface along the 100 ns NVT simulation time. However, the adsorbed macromolecule was more extended on the PLGA surface and spanned the full interfacial width as shown in Figure 4b,c. In the water solution, the DSPE portion of the macromolecule kept closer to the PLGA surface for an extended period of time, while the PEG portion interfaced the water up to a height of ∼2 nm. In contrast, for the solutions with EA the PEG portion of the macromolecule remained closer to the PLGA surface for the overwhelming majority of time, and the DSPE portion reached heights away from the surface as far as 3 nm. Interaction energies between the DSPE-PEG macromolecule and either the PLGA surface or the solvent are given in the

https://doi.org/10.1021/acs.jpcb.1c07490
J. Phys. Chem. B XXXX, XXX, XXX−XXX

Table 4. Interaction Energy between One DSPE-PEG Macromolecule or the Four Macromolecules Droplet with Different Components of the Respective Systems at 300 K[a]

solvent	solute	interacting component	LJ (J/mol)	Coulomb (J/mol)	total (J/mol)
water	macromolecule	PLGA	−29 ± 1	−6 ± 1	−34 ± 2
	macromolecule	solvent	−22 ± 2	−40 ± 3	−63 ± 4
	droplet	PLGA	−72 ± 4	−13 ± 2	−85 ± 5
	droplet	solvent	−77 ± 4	−171 ± 11	−247 ± 13
	droplet	intradroplet	−601 ± 38	−123 ± 19	−724 ± 42
EA	macromolecule	PLGA	−25 ± 2	−6 ± 1	−30.7 ± 2
	macromolecule	solvent	−46 ± 8	−8 ± 2	−55 ± 9
	droplet	PLGA	−72 ± 3	−18 ± 2	−90 ± 4
	droplet	solvent	−250 ± 16	−43 ± 5	−293 ± 19
	droplet	intradroplet	−268 ± 30	−103 ± 24	−370 ± 43
EA/water	macromolecule	PLGA	−15 ± 4	−2 ± 1	−18 ± 5
	macromolecule	solvent	−48 ± 4	−24 ± 3	−72 ± 6
	droplet	PLGA	−59 ± 5	−13 ± 3	−73 ± 7
	droplet	solvent	−171 ± 6	−57 ± 6	−228 ± 9
	droplet	intradroplet	−232 ± 37	−81 ± 24	−313 ± 54

[a]DSPE-PEG macromolecules interacting with themselves within a droplet are listed as intra-interactions. Energies reported are per atom of each system component interacting with either the macromolecule or the droplet. Averages correspond to the last 50 ns for water cases and the last 100 ns for cases involving EA of NVT MD simulations.

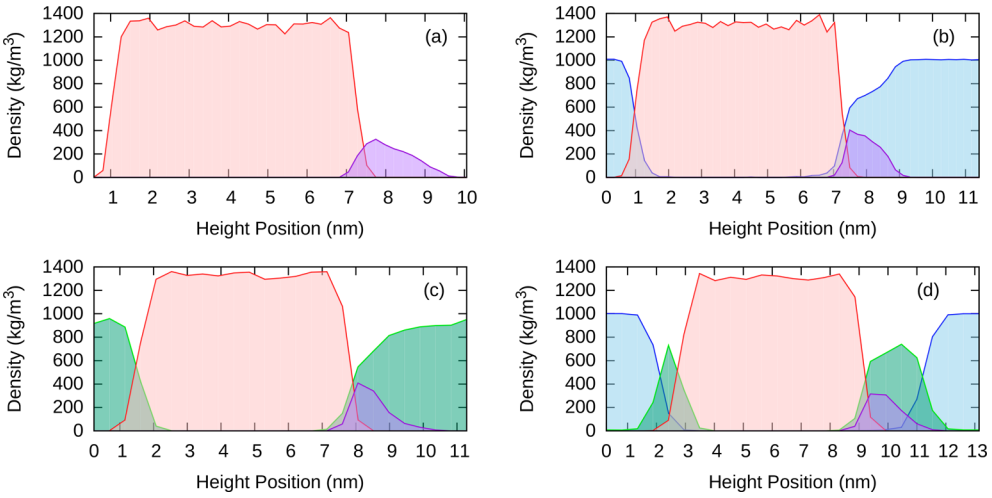

Figure 5. Density profile of PLGA-solvent systems with an adsorbed DSPE-PEG droplet. (a) PLGA-droplet in vacuum, (b). PLGA-droplet in water, (c) PLGA-droplet in EA, (d) PLGA-droplet-mixed solvent. PLGA is depicted in pink, droplet is in magenta, water is in light blue, EA is in green. Data from the NVT simulation at 300 K were averaged over the last 50 ns for water and 100 ns for EA-containing cases.

Table 4. On the one hand, as happened for the isolated solvated macromolecule, when adsorbed on the PLGA surface the interaction energy with the solvent is predominantly of an electrostatic character by 63% in water, contrasting with the dispersive signature of 83% and 66% in the EA and EA/water solvents. On the other hand, the adsorption energy to the PLGA surface is primarily dispersive.

Following the simulation protocol used for the absorption of one DSPE-PEG macromolecule on the PLGA-solvent interface, the four-macromolecule cluster obtained in the vacuum simulation was placed ∼1 nm away from the PLGA surface in three different orientations yielding solutions with 9.8% per mass solute concentration. Systems were NPT equilibrated, and NVT followed for 100 ns. As in the one-macromolecule case, the four-macromolecule cluster adsorbed to the PLGA surface resembling a polymeric droplet-like patch wetting the surface. The assembled PLGA-droplet architecture was employed as the initial structure for simulations with EA and with the EA/water solvents yielding 10.7% and 7.3% per mass solute concentration, respectively. The preformed adsorbed patches emulated kinetically trapped architectures in water that swelled and spread on the solid surface without dissociating while interfacing with EA. A similar droplet-like behavior was observed in the mixed solvent because the PLGA surface interfaces with the EA liquid layer that phase-separated from water. These NVT MD simulations at 300 K were 100 ns long in the water case and 200 ns in the two cases containing EA, displaying very stable total potential energies as shown in Figure S3 of the Supporting Information. In a nutshell, the PLGA surface had a clear adsorbing propensity for patch formation in all three investigated solvents.

Figure 5 shows the density profile of the PLGA-DSPE-PEG interfacing each of the three studied solvents, including the density profile of a PLGA-droplet in vacuum for comparison. The figure depiction conveys clearly that, within the PLGA-solvent interface, there was DSPE-PEG mass aggregation that

https://doi.org/10.1021/acs.jpcb.1c07490
J. Phys. Chem. B XXXX, XXX, XXX−XXX

extended inside the solvent with the highest density accumulated closest to the PLGA surface. Figure 6 illustrates

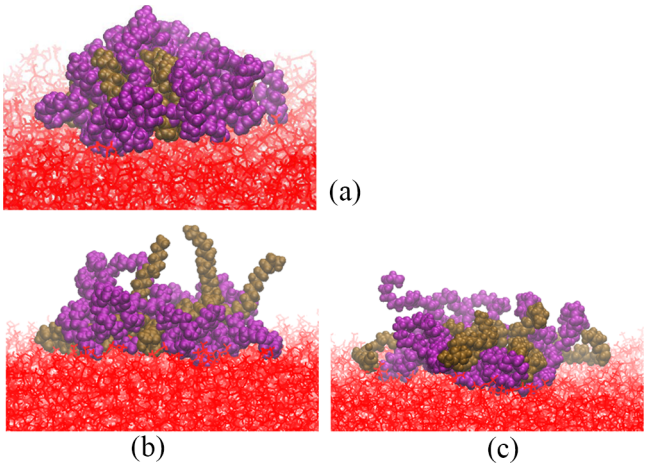

Figure 6. Rendering of the DSPE-PEG droplet-like patches on PLGA surface: (a) in water, (b) in EA; (c) in mixed EA/water. PLGA is colored red, and DSPE-PEG is magenta-ochre. Solvent molecules are not shown. Illustrated is the last configuration of the NVT simulations at 300 K.

the last configuration of the simulations identifying the DSPE-PEG droplet-like patch adsorbed on the PLGA surface in each of the three studied solvents and in vacuum for comparison. Already visually, it is certain that the droplet-like patch formed in water is more compact than those formed in the solvents containing EA. Patches are termed droplets in following paragraphs and sections.

Structural properties of the droplets, averaged over the three simulations, yielded R_g of 3.7 nm in vacuum and water, 4.4 nm in EA, and 3.8 nm in the mixed solvent. Consistently, the SASA was 64, 75, 127, and 129 nm^2 in vacuum, water, EA, and mixed solvent, respectively. Although these properties are not very representative of the droplet shape, they are indicative of clear differences when formed in the different solvents as is additionally evidenced by the PLGA-droplet interaction energy per atom of -724 ± 42, -370 ± 43, and -313 ± 54 J/mol for the water, EA, and mixed solvent, respectively. The dispersion energy (Lennard-Jones) overwhelmingly contributed to these energies over the Coulomb contribution by 83% in water and 73% in the solvents with EA. Table 5 provides a detailed

Table 5. Distribution of Mass within the DSPE-PEG Droplet Height[a]

solvent	water	EA	MIX
$Mass_{0.0-0.5}$ (%)	42 (42)	41 (41)	28 (28)
$Mass_{0.5-1.0}$ (%)	32 (34)	31 (33)	32 (27)
$Mass_{1.0-1.5}$ (%)	22 (20)	21 (21)	30 (23)
$Mass_{1.5-2.0}$ (%)	4 (2)	6 (4)	8 (15)
$Mass_{2.0+}$ (%)	0 (2)	2 (1)	2 (5)
r (nm)	2.18	2.24	2.09
θ (deg)	80.2	80.3	100.4

[a]$Mass_{height}$ is the percent of mass contained within five 0.5 nm droplet slices away from the PLGA surface and, in parentheses, the equivalent percent of volume in the layered sphere cap of the model drop. The fitted circle to the droplet footprint, r, is visualized in Figure 8. The θ values are estimated wetting contact angles (termed θ_b in the Supporting Information Figure S6).

breakdown of the interaction energies of the DSPE-PEG droplet with the different solvents and a comparison with the case of one DSPE-PEG macromolecule affixed to the surface. In the three solvents the droplet adsorption to the PLGA surface is driven by dispersive forces, primarily. However, in the mixed solvent case the adsorption energy is ∼12% less effective, as reported in Table 4. The time evolution of these interaction energies over 100−200 ns is illustrated in the Supporting Information, Figure S4a,b.

The picture that emerged was a swollen droplet of DSPE-PEG material clearly formed on the solid PLGA surface as shown in the rendering of Figure 6. Histograms of the droplet atom heights in the droplet with respect to the PLGA surface are shown in Figure S5 of the Supporting Information. The depiction conveyed that a portion of the droplet PEG component laid on the surface in all three solvent cases creating an adsorption footprint. In the case of water, PEG encapsulated the DSPE shielding it from the water and enabling formation of a hydrophobic core as occurs in larger micelles. However, the droplet core was smashed closer to the surface allowing a thicker coat of PEG interfacing with the water. Meanwhile, in EA the DSPE portion of the droplet tended to position itself further away from the PLGA surface and fully interface with the solvent. Most notably, in the mixed solvent case the droplet resembled the one formed in water with the difference of being asymmetric with a thicker layer of PEG right at the PLGA surface, while the DSPE tended to be distributed as a swollen core enveloped by a thin PEG layer interfaced with the EA/water phase separated solvents.

Another description of the DSPE-PEG droplets of Figure 6 is the inter-macromolecule radial distribution function (rdf) of distances between atoms of different droplet macromolecules depicted in Figure 7. Regardless of solvent, each DSPE-PEG

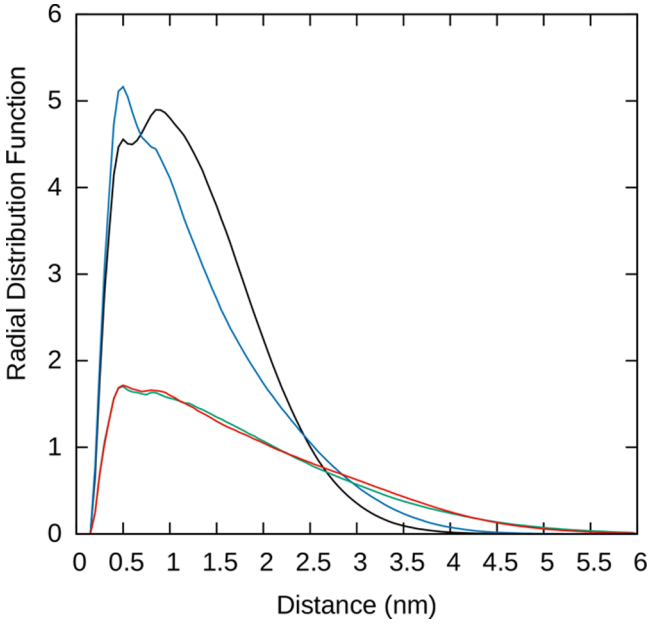

Figure 7. Radial distribution functions of DSPE-PEG droplets formed onto the PLGA surface of atom−atom distances between macromolecules composing the droplet at 300 K. Droplet in vacuum (black), in water (blue), in EA (green), and in the EA/water mixed solvent (red). Data were averaged over the last 50 ns for water and the last 100 ns for EA solutions of NVT MD simulations. A fixed volume of 6^3 nm^3 was used in the normalization.

https://doi.org/10.1021/acs.jpcb.1c07490
J. Phys. Chem. B XXXX, XXX, XXX−XXX

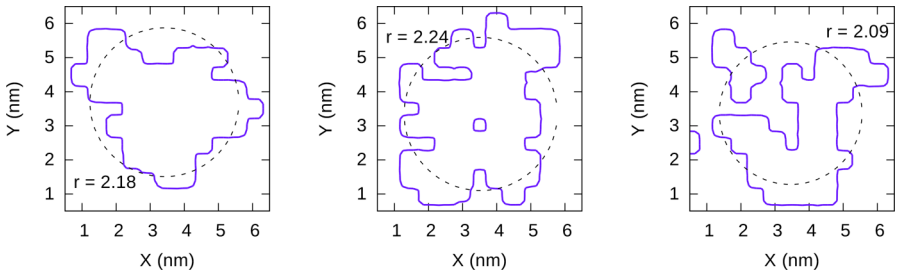

Figure 8. Footprint of the DSPE-PEG droplet on top of the PLGA surface in water (left), EA (middle), and mixed solvent (right) depicted in Figure 6. Circles and their radii r (in nm) characterize the droplet/surface contact area on the average along the last 20 ns of NVT MD data at 300 K.

droplet developed a first coordination shell at ∼0.5 nm, a second peak between 0.8 and 0.85 nm, and extended ∼3.5 nm. In contrast, the droplet rdf in EA and EA/water solvents did not display a structure and extended over more than 5 nm, while water had a compacting effect.

f8 **3.4. Surface Wetting by DSPE-PEG Droplets.** Figure 8 shows the DSPE-PEG droplet footprint made on the PLGA surface. This footprint was defined as a contour plot accounting for the DSPE-PEG droplet mass encountered within 0.5 nm height from the PLGA surface. The surface was not perfectly flat; it was, however, approximately flat and within the resolution for defining the contours. The footprint area was fitted by the best circle through a nonlinear regression; such a circle is shown in Figure 8. The droplet mass located in additional cross section slides of height 0.5 nm above the footprint was also monitored as reported in Table 5.

Wetting is the ability of liquids to maintain contact with a solid surface caused by molecular forces,[47] which promotes the formation of liquid drops for a small amount of liquid. This mechanism is characterized by a wetting contact angle identifying the degree of drop spreading on a planar surface. A liquid drop forming a perfect hemisphere on a planar surface would have a contact angle of 90°, which would turn acute the more flushed the liquid is against the surface or obtuse when the drop would pull away from the surface. Proposing that the DSPE-PEG droplet structure be ideally enveloped by a hemisphere cup that sits on a surface (Figure S6 of the Supporting Information), its circular base was assigned to be the best-fitted circle to the DSPE-PEG footprint depicted in Figure 8 and reported in Table 5. Then, a wetting contact angle was identified as the angle that the enveloping sphere cap made with the surface. The cap height was determined by partitioning the spherical enveloping cap into five slices parallel to its circular base and equating their volumes to the distribution of droplet mass obtained from the simulations and listed in Table 5. The idealized enveloping model predicted an acceptable surface contact for droplets formed within the interface PLGA-pure solvent. However, the case of the smeared, weakly adsorbed droplet in the mixed solvent was characterized by an obtuse contact angle. Thus, from the droplet mass distribution a guiding, not perfect, estimate to the droplet wetting contact angles yielded an additional metrics of the DSPE-PEG droplet formation.

Experimentally,[8,12,13] the synthesis of PLGA nanoparticles with DSPE-PEG patches required a high-shear mixing of a DSPE-PEG aqueous solution aliquot with the PLGA-EA solution in order for the DSPE-PEG patches to form. Therefore, we envision that the formation of droplets occurs only when water-solvated DSPE-PEG structures hit the nanoparticle surface and enough water is flowing in that area for enabling the macromolecular adsorption.

Summarizing, among the three solvents environments investigated, the most compact DSPE-PEG droplet atop the PLGA surface occurs at the PLGA-water interface, as illustrated in Figures 5−7. In contrast, the DSPE-PLGA droplet in the presence of the mixed EA/water solvent resembles a smeared patch affixed to the surface as evidenced in the density profile of Figure 5 that shows a droplet extending over approximately twice the PLGA-solvent interface width.

4. CONCLUSION

This de novo research presents an atomistic characterization of the interface between a PLGA glassy surface and three solvents, namely, water, ethyl acetate, and the mixture of them. Moreover, the mechanism of PEGylating the solid surface with DSPE-PEG macromolecular droplets that resemble patches is evidenced at the nanoscale. We have followed the formation of 3−6 nm DSPE-PEG droplets that adsorb onto the PLGA surface and characterized their shape, size, and mass distribution emphasizing the peculiarities due to the different solvents. The droplet shapes resemble hemispheres while at the PLGA-water interface and smear out on the surface and into the solvent at the PLGA-ethyl acetate interface. Energetic analyses of droplet-PLGA and droplet-solvent show that dispersive forces are dominant in the droplet adhesion to the surface while electrostatic forces are dominant in water for keeping the surface decorating droplet formations more hemispherical. A novel approach using a three-dimensional (3D) contour analysis and droplet mass distribution enabled estimates of the droplet wetting contact angles to the PLGA surface predicting a significantly more enhanced wetting ability from droplets formed at the PLGA-water interface than those assembled at the PLGA-ethyl acetate interface. Looked at from far away, these droplets have the appearance of patches.

Nanoparticles exhibiting a patch type of surface decoration have peculiar optical and electronic properties amenable to a specific tailoring of their assemblies in therapeutic applications. In fact, droplet-decorated and asymmetric nanoparticles have potential applications in fundamental research, sensing, diagnosis, and the self-assembly and stabilization of polymeric nanoarchitectures. Our pioneering work provides a foundation for future research on other polymer−lipid nanostructures, such as the formation of micelles, vesicles, monolayers, and bilayers interfacing nanoparticles of different polymeric content. Recent advances in self-assembly experimental automation[48−50] are compelling opportunities for expanding more broadly the approach put forward in our in silico work.

https://doi.org/10.1021/acs.jpcb.1c07490
J. Phys. Chem. B XXXX, XXX, XXX−XXX

■ ASSOCIATED CONTENT

Supporting Information

The Supporting Information is available free of charge at https://pubs.acs.org/doi/10.1021/acs.jpcb.1c07490.

Content: Visualization of the DSPE-PEG macromolecule and its calculated RESP atomic charges for the GAFF/Lipids17 combined force field. Plots of the ternary and quaternary PLGA+DSPE-PEG+solvent total potential energy at 300 K along the NVT MD simulation time. Droplet interaction energies with the PLGA surface and with the solvents as a function of time at 300 K. Histograms of atom heights within the adsorbed droplets measured with respect to the PLGA surface interfacing the three solvents. The estimate of droplet wetting contact angles is supported with geometric definitions. 452 custom-generated RESP charges used in the combined GAFF/Lipids17 for modeling the DSPE-PEG polymer−lipid macromolecule (PDF)

■ AUTHOR INFORMATION

Corresponding Author

Estela Blaisten-Barojas − *Center for Simulation and Modeling (formerly, Computational Materials Science Center) and Department of Computational and Data Sciences, George Mason University, Fairfax, Virginia 22030, United States;* orcid.org/0000-0003-3259-1573; Email: blaisten@gmu.edu

Author

James Andrews − *Center for Simulation and Modeling (formerly, Computational Materials Science Center) and Department of Computational and Data Sciences, George Mason University, Fairfax, Virginia 22030, United States*

Complete contact information is available at: https://pubs.acs.org/10.1021/acs.jpcb.1c07490

Notes

The authors declare no competing financial interest.

■ ACKNOWLEDGMENTS

We acknowledge partial support from the Commonwealth of Virginia (United States) 4-VA Grant No. 331050. J.A. is thankful to the Provost Office of George Mason University for the presidential scholarship support. All computations were done in Argo, the supercomputer cluster of the Office for Research Computing at George Mason University.

■ REFERENCES

(1) Ghitman, J.; Biru, E. I.; Stan, R.; Iovu, H. Review of Hybrid PLGA Nanoparticles: Future of Smart Drug Delivery and Theranostics Medicine. *Mater. Des.* **2020**, *193*, 108805.

(2) Bose, R. J.; Lee, S.-H.; Park, H. Lipid-Based Surface Engineering of PLGA Nanoparticles for Drug and Gene Delivery Applications. *Biomater Res.* **2016**, *20*, 34.

(3) Kumari, A.; Yadav, S. K.; Yadav, S. C. Biodegradable Polymeric Nanoparticles Based Drug Delivery Systems. *Colloids Surf., B* **2010**, *75*, 1−18.

(4) Zhang, L.; Chan, J. M.; Gu, F. X.; Rhee, J.-W.; Wang, A. Z.; Radovic-Moreno, A. F.; Alexis, F.; Langer, R.; Farokhzad, O. C. Self-Assembled Lipid-Polymer Hybrid Nanoparticles: a Robust Drug Delivery Platform. *ACS Nano* **2008**, *2*, 1696−1702.

(5) Mu, Q.; Hu, T.; Yu, J. Molecular Insight into the Steric Shielding Effect of PEG on the Conjugated Staphylokinase: Biochemical Characterization and Molecular Dynamics Simulation. *PLoS One* **2013**, *8*, e68559.

(6) Bailon, P.; Berthold, W. Polyethylene Glycol-Conjugated Pharmaceutical Proteins. *Pharm. Sci. Technol. Today* **1998**, *1*, 352−356.

(7) Milla, P.; Dosio, F.; Cattel, L. PEGylation of Proteins and Liposomes: a Powerful and Flexible Strategy to Improve the Drug Delivery. *Curr. Drug Metab.* **2012**, *13*, 105−119.

(8) Salvador-Morales, C.; Brahmbhatt, B.; Marquez-Miranda, V.; Araya-Duran, I.; et al. Mechanistic Studies on the Self-Assembly of PLGA Patchy Particles and Their Potential Applications in Biomedical Imaging. *Langmuir* **2016**, *32*, 7929−7942.

(9) Hadinoto, K.; Sundaresan, A.; Cheow, W. S. Lipid-Polymer Hybrid Nanoparticles as a New Generation Therapeutic Delivery Platform: a Review. *Eur. J. Pharm. Biopharm.* **2013**, *85*, 427−443.

(10) Aguilar-Castillo, B. A.; Santos, J. L.; Luo, H.; Aguirre-Chagala, Y. E.; Palacios-Hernández, T.; Herrera-Alonso, M. Nanoparticle Stability in Biologically Relevant Media: Influence of Polymer Architecture. *Soft Matter* **2015**, *11*, 7296−7307.

(11) Vukovic, L.; Khatib, F. A.; Drake, S. P.; Madriaga, A.; Brandenburg, K. S.; Král, P.; Onyuksel, H. Structure and Dynamics of Highly PEGylated Sterically Stabilized Micelles in Aqueous Media. *J. Am. Chem. Soc.* **2011**, *133*, 13481−13488.

(12) Rasheed, N.; Khorasani, A.; Cebral, J.; Mut, F.; Lohner, R.; Salvador-Morales, C. Mechanisms Involved in the Formation of Biocompatible Lipid Polymeric Hollow Patchy Particles. *Langmuir* **2015**, *31*, 6639−6648.

(13) Salvador-Morales, C.; Valencia, P. M.; Gao, W.; Karnik, R.; Farokhzad, O. C. Spontaneous Formation of Heterogeneous Patches on Polymer-Lipid Core-Shell Particle Surfaces During Self-Assembly. *Small* **2013**, *9*, 511−517.

(14) Persano, F.; Gigli, G.; Leporatti, S. Lipid-polymer Hybrid Nanoparticles in Cancer Therapy: Current Overview and Future Directions. *Nano Express* **2021**, *2*, 012006.

(15) Sponseller, D.; Blaisten-Barojas, E. Solutions and Condensed Phases of PEG_{2000} from All-Atom Molecular Dynamics. *J. Phys. Chem. B* **2021**, *125*, 12892−12901.

(16) Andrews, J.; Blaisten-Barojas, E. Exploring with Molecular Dynamics the Structural Fate of PLGA Oligomers in Various Solvents. *J. Phys. Chem. B* **2019**, *123*, 10233−10244.

(17) Andrews, J.; Handler, R. A.; Blaisten-Barojas, E. Structure, Energetics and Thermodynamics of PLGA Condensed Phases from Molecular Dynamics. *Polymer* **2020**, *206*, 122903.

(18) Gentile, P.; Chiono, V.; Carmagnola, I.; Hatton, P. An Overview of Poly(lactic-co-glycolic) Acid (PLGA)-Based Biomaterials for Bone Tissue Engineering. *Int. J. Mol. Sci.* **2014**, *15*, 3640−3659.

(19) Lanao, R. F.; Jonker, A.; Wolke, J.; Jansen, J.; van Hest, J.; Leeuwenburgh, S. Physicochemical Properties and Applications of Poly(lactic-co-glycolic acid) for Use in Bone Regeneration. *Tissue Eng., Part B* **2013**, *19*, 380−390.

(20) Gilding, D.; Reed, A. Biodegradable Polymers for Use in Surgery - Polyglycolic/polylactic Acid Homo- and Copolymers: 1. *Polymer* **1979**, *20*, 1459−1464.

(21) Wang, J.; Wolf, R. M.; Caldwell, J. W.; Kollman, P. A.; Case, D. A. Development and Testing of a General AMBER Force Field. *J. Comput. Chem.* **2004**, *25*, 1157−1174.

(22) Bayly, C. I.; Cieplak, P.; Cornell, W.; Kollman, P. A. A Well-Behaved Electrostatic Potential Based Method Using Charge Restraints for Deriving Atomic Charges: the RESP Model. *J. Phys. Chem.* **1993**, *97*, 10269−10280.

(23) Dickson, C. J.; Madej, B. D.; Skjevik, A.; Betz, R. M.; Teigen, K.; Gould, I. R.; Walker, R. C. Lipid14: the AMBER Lipid Force Field. *J. Chem. Theory Comput.* **2014**, *10*, 865−879.

(24) Singh, U. C.; Kollman, P. A. An Approach to Computing Electrostatic Charges for Molecules. *J. Comput. Chem.* **1984**, *5*, 129−145.

(25) Besler, B. H.; Merz, K. M., Jr.; Kollman, P. A. Atomic Charges Derived from Semiempirical Methods. *J. Comput. Chem.* **1990**, *11*, 431−439.
(26) Frisch, M. J.; Trucks, G. W.; Schlegel, H. B.; Scuseria, G. E.; Robb, M. A.; Cheeseman, J. R.; Scalmani, G.; Barone, V.; Mennucci, B.; Petersson, G. A.; et al. *Gaussian 09,* rev. E.01; Gaussian, Inc.: Wallingford, CT, 2009.
(27) AMBER 2018 Reference Manual (Covers AmberTools18). https://ambermd.org/doc12/Amber18.pdf, accessed 2021-10-12.
(28) Wang, J.; Wang, W.; Kollman, P. A.; Case, D. A. Automatic Atom Type and Bond Type Perception in Molecular Mechanical Calculations. *J. Mol. Graphics Modell.* **2006**, *25*, 247−260.
(29) Welcome to the GROMACS Documentation. https://manual.gromacs.org/documentation/2020/index.html, accessed 2021-10-12.
(30) Shirts, M. R.; Klein, C.; Swails, J. M.; Yin, J.; Gilson, M. K.; Mobley, D. L.; Case, D. A.; Zhong, E. D. Lessons Learned from Comparing Molecular Dynamics Engines on the SAMPL5 Dataset. *J. Comput.-Aided Mol. Des.* **2017**, *31*, 147−161.
(31) Schauperl, M.; Nerenberg, P. S.; Jang, H.; Wang, L.-P.; Bayly, C. I.; Mobley, D. L.; Gilson, M. K. Non-bonded Force Field Model with Advanced Restrained Electrostatic Potential Charges (RESP2) *Comms. Chem.* **2020**, *3*. DOI: 10.1038/s42004-020-0291-4
(32) Berendsen, H.; Grigera, J.; Straatsma, T. The Missing Term in Effective Pair Potentials. *J. Phys. Chem.* **1987**, *91*, 6269−6271.
(33) Andrews, J.; Blaisten-Barojas, E. Workflow for Investigating Thermodynamic, Structural and Energy Properties of Condensed Polymer Systems In *Advances in Parallel & Distributed Processing and Applications: CSCE'20 Proceedings*; Arabnia, H. R., Deligiannidis, L., Grimaila, M. R., Hodson, D. D., Joe, K., Sekijima, M., Tinetti, F. G., Eds.; Springer Nature: NY, 2021; pp 1033−1039. DOI: 10.1007/978-3-030-69984-0_75
(34) Van Der Spoel, D.; Lindahl, E.; Hess, B.; Groenhof, G.; Mark, A. E.; Berendsen, H. J. C. GROMACS: Fast, Flexible, and Free. *J. Comput. Chem.* **2005**, *26*, 1701−18.
(35) Hess, B.; Kutzner, C.; van der Spoel, D.; Lindahl, E. GROMACS 4: Algorithms for Highly Efficient, Load-Balanced, and Sscalable Molecular Simulation. *J. Chem. Theory Comput.* **2008**, *4*, 435−447.
(36) Abraham, M.; Murtola, T.; Schulz, R.; Páll, S.; Smith, J.; Hess, B.; Lindahl, E. GROMACS: High Performance Molecular Simulations Through Multi-Level Parallelism from Laptops to Supercomputers. *SoftwareX* **2015**, *1−2*, 19−25.
(37) Darden, T.; York, D.; Pedersen, L. Particle Mesh Ewald: an N log(N) Method for Ewald Sums in Large Systems. *J. Chem. Phys.* **1993**, *98*, 10089−10092.
(38) Degradex®, PLGA Microspheres and PLGA Nanoparticles. https://www.degradex.com/degradexreg-plga-microspheres.html, accessed 2021-10-12.
(39) Bussi, G.; Donadio, D.; Parrinello, M. Canonical Sampling Through Velocity Rescaling. *J. Chem. Phys.* **2007**, *126*, 014101.
(40) Berendsen, H. J. C.; Postma, J. P. M.; van Gunsteren, W. F.; DiNola, A.; Haak, J. R. Molecular Dynamics with Coupling to an External Bath. *J. Chem. Phys.* **1984**, *81*, 3684−3690.
(41) Parrinello, M.; Rahman, A. Polymorphic Transitions in Single Crystals: A New Molecular Dynamics Method. *J. Appl. Phys.* **1981**, *52*, 7182−7190.
(42) Nosé, S.; Klein, M. Constant Pressure Molecular Dynamics for Molecular Systems. *Mol. Phys.* **1983**, *50*, 1055−1076.
(43) Usatenko, Z.; Sommer, J.-U. Calculation of the Segmental Order Parameter for a Polymer Chain in Good Solvent. *Macromol. Theory Simul.* **2008**, *17*, 39−44.
(44) Dai, Y.; Blaisten-Barojas, E. Monte Carlo Study of Oligopyrroles in Condensed Phases. *J. Chem. Phys.* **2010**, *133*, 034905.
(45) Israelachvili, J. N. *Intermolecular and Surface Forces,* 3rd ed.; Academic Press: San Diego, CA, 2011; pp 535−576 DOI: 10.1016/C2009-0-21560-1.
(46) Che, J.; Okeke, C. I.; Hu, Z.-B.; Xu, J. DSPE-PEG: A Distinctive Component in Drug Delivery System. *Curr. Pharm. Des.* **2015**, *21*, 1598−1605.
(47) .Zisman, W. A. Relation of the Equilibrium Contact Angle to Liquid and Solid Constitution. In *Contact Angle, Wettability, and Adhesion;* Advances in Chemistry Series; Fowkes, F. M., Ed.; American Chemical Society, 1964; Vol. *43*; pp 1−51 DOI: 10.1021/ba-1964-0043.ch001.
(48) Wessels, M. G.; Jayaraman, A. Computational Reverse-Engineering Analysis of Scattering Experiments (CREASE) on Amphiphilic Block Polymer Solutions: Cylindrical and Fibrillar Assembly. *Macromolecules* **2021**, *54*, 783−796.
(49) Vena, M. P.; de Moor, D.; Ianiro, A.; Tuinier, R.; Patterson, J. P. Kinetic State Diagrams for a Highly Asymmetric Block Copolymer Assembled in Solution. *Soft Matter* **2021**, *17*, 1084.
(50) Parent, L. R.; Bakalis, E.; Ramirez-Hernández, A.; Kammeyer, J. K.; Park, C.; de Pablo, J.; Zerbetto, F.; Patterson, J. P.; Gianneschi, N. C. Directly Observing Micelle Fusion and Growth in Solution by Liquid- Cell Transmission Electron Microscopy. *J. Am. Chem. Soc.* **2017**, *139*, 17140−17151.

https://doi.org/10.1021/acs.jpcb.1c07490
J. Phys. Chem. B XXXX, XXX, XXX−XXX